Molecular Vision 2021; 27:679-690 <http://www.molvis.org/molvis/v27/679>
Received 17 June 2021 | Accepted 5 December 2021 | Published 7 December 2021

Lacrimal gland homeostasis is maintained by the *AQP5* pathway by attenuating endoplasmic reticulum stress inflammation in the lacrimal gland of *AQP5* knockout mice

Shaohua Hu,[1] Guohu Di,[1,3] Xin Cao,[1] Yaning Liu,[1] Yihui Wang,[1] Hui Zhao,[4] Dianqiang Wang,[2] Peng Chen[1,3]

(The first two authors contributed equally to this article.)

[1]Department of Human Anatomy, Histology and Embryology, School of Basic Medicine, Qingdao University, Qingdao, Shandong Province, China; [2]Qingdao Aier Eye Hospital, Qingdao, China; [3]Institute of Stem Cell Regeneration Medicine, School of Basic Medicine, Qingdao University, Qingdao, China; [4]The 971 Hospital of the Chinese People's Liberation Army Navy, Qingdao, Shandong Province, China

Purpose: AQP5$^{-/-}$ mice spontaneously exhibit dry eye symptoms. The purpose of this study was to assess the endoplasmic reticulum (ER) stress-mediated inflammation generated by a deficiency of aquaporin 5 (AQP5) in the lacrimal gland.
Methods: Hematoxylin and eosin (H&E) staining, Oil Red O staining, and transmission electron microscopy (TEM) analysis were performed to identify structural changes in lacrimal gland epithelial cells because of AQP5 deficiency. Corneal epithelial defects were assessed with sodium fluorescein staining. The expression profiles of mRNA and proteins were determined by quantitative real-time reverse transcription PCR (qRT-PCR) and western blot. Mice in the quercetin group were injected intraperitoneally with 40 mg/kg of quercetin, and the control group was injected with an equal volume of dimethyl sulfoxide (DMSO) for 4 weeks.
Results: Aqueous tear secretion fell at about 50% in 1- and 6-month-old AQP5$^{-/-}$ mice compared with that of AQP5$^{+/+}$ mice. TEM showed that the ER structure was damaged. ER stress was significantly increased in the lacrimal gland of AQP5$^{-/-}$ mice. Lipid droplets accumulated in the matrix and acinar cells, and changes occurred in the lipid metabolism and gene expression levels for *PPARα*, *CPT1α*, and *CPT2* in the AQP5$^{-/-}$ mice. Immune cell infiltration and increases in the gene expression levels of the chemokines *CXCL1*, *CXCL2*, and *CCL5* were found in the lacrimal gland of AQP5$^{-/-}$ mice. Quercetin partially reversed ER stress levels, inflammation, and lipid accumulation, and it inhibited tear secretion.
Conclusions: The study data indicated that a deficiency of AQP5 induced pathophysiological changes and functional decompensation of the lacrimal gland. Quercetin may improve the inflammation in the lacrimal glands of AQP5$^{-/-}$ mice by regulating the ER stress levels.

The lacrimal gland is the organ that secretes tears, which are essential for the lubrication of the eye. Disruption of lacrimal fluid composition, production, or release results in dry eye, causing discomfort and damage to the ocular surface [1]. The lacrimal gland consists of the acini, ducts, nerves, myoepithelial cells (MECs), and plasma cells [2,3]. Acinar cells compose about 80% of the glands and secrete electrolytes, water, and proteins to form primary fluid. As the primary fluid moves along the duct system, the duct cells modify the primary fluid by secreting or absorbing electrolytes. The final lacrimal gland fluid is then secreted onto the surface of the eye. Lacrimal gland secretion is primarily under neural control, which is achieved through a neural reflex arc [4]. A decrease or lack of lacrimal gland secretion is the leading cause of aqueous tear–deficient dry eye syndrome [5]. Many causes, including autoimmune diseases (e.g., Sjögren syndrome [SS]) [6], allogeneic hematopoietic cell transplantation [7], ligation of the lacrimal gland duct [8], and aging [9], can induce lacrimal gland damage. These injuries can result in sufficient lacrimal gland malfunction to cause dry eye disease.

The endoplasmic reticulum (ER) is a dynamic cell lumen. Its main functions are secretion, synthesis, and folding of transmembrane proteins and regulation of calcium balance [10]. ER stress has been described in many diseases, including rheumatoid arthritis, neurodegenerative diseases, cardiovascular disorders, and inflammatory bowel disease [11,12]. Recently, it has been found that ER stress may be a pathophysiological change in the conjunctival pathogenesis of dry eye syndrome [13].

At the same time, inflammatory infiltration and fibrosis of lacrimal gland tissue could decrease tear secretion and eventually lead to dry eye [14]. Lipid metabolism involves the

Correspondence to: Peng Chen, Department of Human Anatomy, Histology and Embryology, School of Basic Medicine, Qingdao University, 308 Ningxia Road, Qingdao 266071, China; Phone: (532) 8378-0061; FAX: (532) 83780081; email: chenpeng599205@126.com.

synthesis and degradation of lipids in cells [15,16]. The ER is the major organelle involved in lipid metabolism because it contains many relevant enzymes for this process. ER stress is a potential mechanistic link between excess nutrients and lipid accumulation, which is a crucial event in the development of minor labial salivary gland tissue [17,18]. It has also been shown that lymphocytic infiltration destruction of the acini increases with age, and abnormal lipid metabolism has been found in the lacrimal gland of a sleep deprivation–induced mouse dry eye model [19].

Thirteen known aquaporins (AQPs) are widely distributed in various organs and play different roles in the body. AQP5 has been detected in the salivary glands, lacrimal glands, cornea, and lungs [20]. In the salivary glands, AQP5 is localized at the apical membrane of serous-type acinar cells [21]. AQP5 knockout studies in mice confirm the critical role of AQP5 in water secretion in salivary gland acinar cells [22,23]. It has been proposed that AQP5 abnormalities may occur in SS and that aquaporin gene delivery to the lacrimal and salivary glands could increase fluid secretion.

Quercetin is a known phytochemical with antioxidant and anti-inflammatory properties [24,25]. It has been reported to directly inhibit the reactive oxygen species (ROS)-promoted activation of nuclear factor-κB (NF-κB) signaling [26,27]. Moreover, topical application of quercetin seems to suppress inflammation of the ocular surface and lacrimal gland [28]. The anti-inflammatory effect of quercetin has been reported in several studies, and dry eye can be effectively controlled in mice after alleviating lacrimal gland inflammation [29]. Found in natural botanical plants, quercetin is under basic and early stage clinical research for a variety of disease conditions [30]. It can protect RAW264.7 macrophages from glucosamine-induced lipid accumulation through the suppression of ER stress, as evidenced by reduced C/EBP homologous protein (CHOP) and activating transcription factor-6 (ATF6) levels [31]. We analyzed the anti-inflammatory effects and mechanisms of quercetin on ER stress-mediated inflammation raised by a deficiency of AQP5 in the lacrimal gland. Our results showed that in the lacrimal glands of AQP5$^{-/-}$ mice, ER stress and its induced inflammation were present in lacrimal epithelial cells, as was abnormal lipid metabolism. Quercetin partially reversed the

Table 1. The primers used in qRT-PCR.

Gene	Primer type	Primer sequence
CPT1α	Forward	CTTCCAACGCATGACAGCAC
	Reverse	TTAACCATGATCGGCCCTCG
CPT2	Forward	GAGGCATTTGTCAGGGAGCC
	Reverse	CTGCTGCCAGATACCGTAGAG
PPARα	Forward	GAACCGGAACAAATGCCAGT
	Reverse	CTTCAGGTAGGCTTCGTGGA
MCP-1	Forward	CAGCAAGATGATCCCAATGAGTAG
	Reverse	TTTTTAATGTATGTCTGGACCCATTC
CXCL1	Forward	CGCTTCTCTGTGCAGCGCTGCTGCT
	Reverse	AAGCCTCGCGACCATTCTTGAGTC
CXCL2	Forward	CCTGGTTCAGAAAATCATCCA
	Reverse	CTTCCGTTGAGGGACAGC
CCL5	Forward	TTCCCTGTCATCGCTTGCTCT
	Reverse	CGGATGGAGATGCCGATTTT
IL-1β	Forward	CTTTCCCGTGAACCTTCCA
	Reverse	CTCGGAGCCTGTAGTGCAGTT
IL-6	Forward	ACCACTCCCAACAGACCTGTCT
	Reverse	TCAGATTGTTTTCTGCAAGTGCAT
TNF-α	Forward	ACAAGGCTGCCCCGACTAC
	Reverse	CTGGGCTCATACCAGGGTTTG
GAPDH	Forward	GCCACCCAGAAGACTGTGGAT
	Reverse	CTCGGAGCCTGTAGTGCAGTT

inhibited ER stress levels, lipid accumulation, inflammation, and tear secretion.

METHODS

Animals: Using clustered regularly interspaced short palindromic repeat - associated Cas9 (CRISPR/Cas9) technology, AQP5$^{-/-}$ mice were produced by the high-flux electric transfer of fertilized eggs from Cyagen Biosciences Inc. (Guangzhou, China) [32]. Age-matched AQP5$^{+/+}$ and AQP5$^{-/-}$ mice were used for our study. Six-month-old AQP5$^{-/-}$ mice were divided into quercetin and control groups (n = 7 per group). Quercetin (purity ≥98%, Sigma, St. Louis, MO) was dissolved in dimethyl sulfoxide (DMSO; 100%; Solarbio, Beijing, China) at 100 mg/ml. Mice were injected intraperitoneally with quercetin in DMSO in the quercetin group (40 mg/kg, 7 µl per mouse) or DMSO alone in the control group (100% DMSO, 7 µl per mouse) once per day for 4 weeks.

TEM: Transmission electron microscopy (TEM) was conducted as described previously [33]. In brief, the lacrimal glands were cut into 1 mm^3 blocks and fixed in prechilled 2.5% glutaraldehyde. After fixing and dehydration, the sections were double-stained with uranium and lead and observed under a transmission electron microscope (HITACHI, Tokyo, Japan).

Tear measurements and corneal fluorescein staining: Tears were measured by inserting cotton phenol red threads (Zone-Quick, AYUMI Pharmaceutical, Tokyo, Japan) into the lateral canthus of the eye for 20 s in unanesthetized animals, as described previously [33]. A 1% fluorescein solution (Sigma) was applied to the cornea for 2 min. The eyes were rinsed with PBS and examined using a cobalt blue light from a slit-lamp scope (66 Vision Tech. Co., Ltd., Suzhou, China).

H&E and immunofluorescence staining: Mice were sacrificed by cervical dislocation, and the lacrimal glands were fixed in 10% buffered formalin and embedded in paraffin. Paraffin sections (4 µm) were stained with hematoxylin and eosin (H&E) and observed under a light microscope (CKX53, Olympus, Tokyo, Japan). Lacrimal gland cryosections (6 µm) were fixed in 4% paraformaldehyde and then immunostained with anti-AQP5 antibody (1:100, Abcam, Cambridge, UK) and anti-α-smooth muscle actin (anti-α-SMA; 1:100, Abcam). The samples were then incubated with secondary

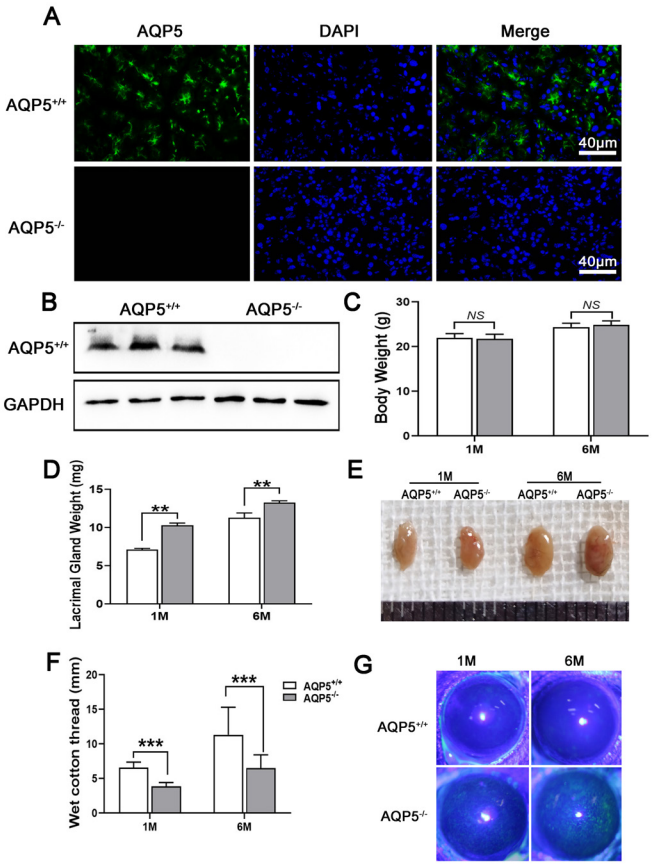

Figure 1. AQP5 deficiency induced dry eye–like characteristics. **A**: Immunofluorescence staining showed the expression of AQP5 in the lacrimal gland cell location (green: AQP5, blue: 4'6-diamidino-2-phenylindole [DAPI]). **B**: Expression of AQP5 and GAPDH were examined by western blotting. **C**: Bodyweight (n = 10 samples). **D**: Lacrimal gland weight and **E**: appearance (n = 8 samples). **F**: Tear secretion of AQP5$^{+/+}$ mice and AQP5$^{-/-}$ mice. **G**: Sodium fluorescein staining of AQP5$^{+/+}$ mice and AQP5$^{-/-}$ mice. Scale bars: (**A**) 40 µm. * p<0.05, ** p<0.01, *** p<0.0001.

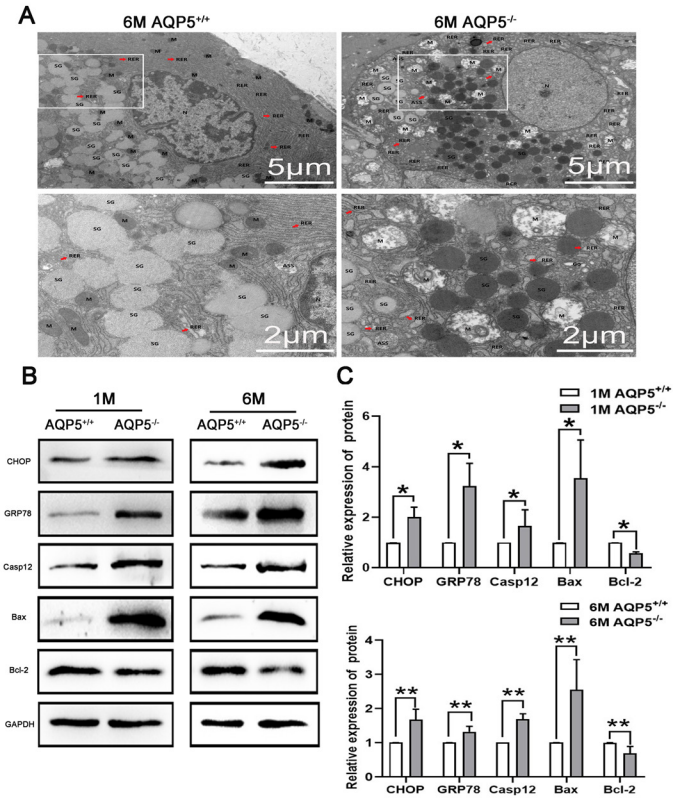

Figure 2. AQP5 deficiency induced ultrastructural abnormalities and endoplasmic reticulum (ER) stress in the lacrimal gland. **A**: Transmission electron microscopy (TEM) showing the ultrastructure of the acinar cells of the lacrimal gland. Data are expressed as mean ± standard deviation (SD). *p<0.05, **p<0.001. Scale bars: (**A**) 5 μm, 2 μm. **B**: The deficiency of AQP5 protein induced endoplasmic reticulum stress in lacrimal glands of mice. Western blot bands for CHOP, GRP78, Caspase12, Bax, Bcl-2, and GAPDH (n = 3 samples). **C**: Quantified intensities of western blot bands for CHOP, GRP78, Caspase12, Bax, and Bcl-2 compared with GAPDH (n = 3 samples). *p<0.05, **p<0.01, *** p<0.0001.

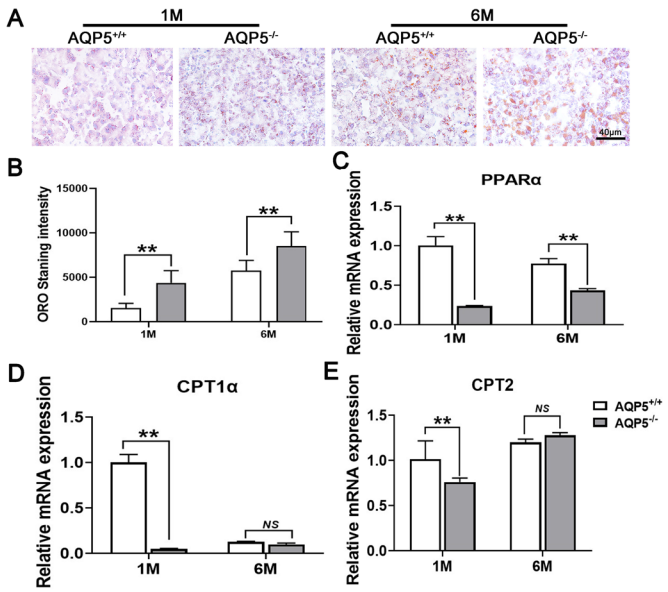

Figure 3. AQP5$^{-/-}$ induced abnormal lipid metabolism in the lacrimal gland. **A**: Oil Red O (ORO) staining (n = 6 samples). **B**: ORO staining intensity analyzed by ImageJ software (n = 6 samples). **C**,**D**,**E**: Real-time PCR analyzed the expression of *PPARα*, *CPT1α*, and *CPT2* (n = 3 samples). *p<0.05, **p<0.001, two-way analysis of variance (ANOVA). Scale bars: (A) 40 μm. * p<0.05, ** p<0.01, *** p<0.0001.

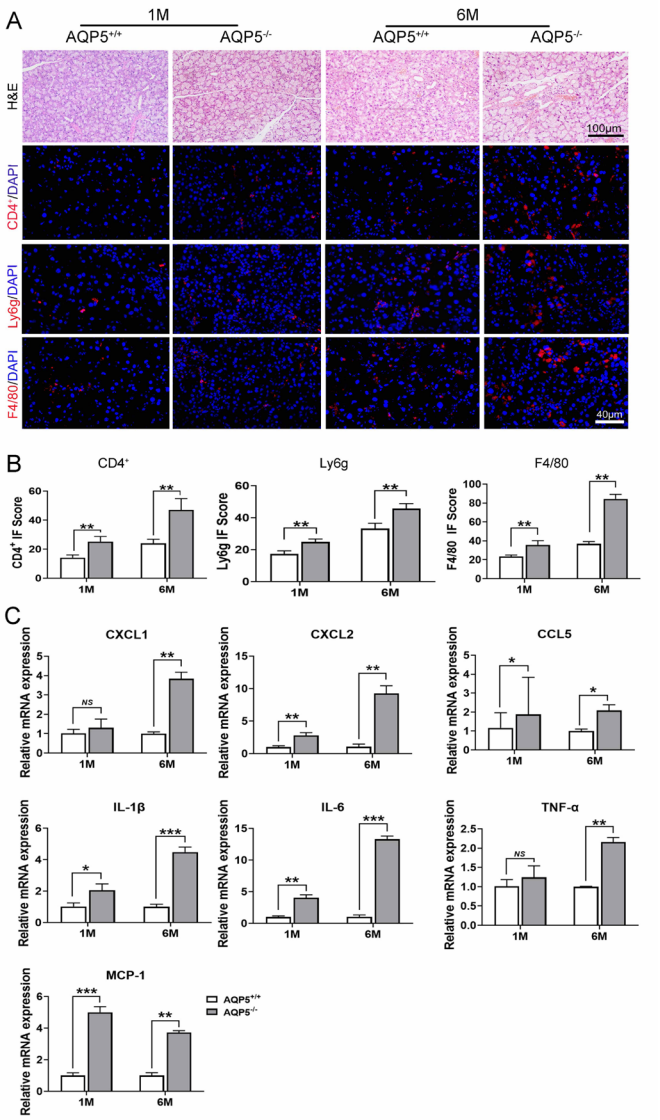

Figure 4. AQP5 deficiency induced inflammation in the lacrimal gland. **A**: Hematoxylin and eosin (H&E) staining showed morphology changes. $CD4^+$: Immunofluorescence staining of $CD4^+$ demonstrated $CD4^+$ T cells (red: $CD4^+$, blue: 4'6-diamidino-2-phenylindole [DAPI]). Ly6g: Immunofluorescence staining of Ly6g showed neutrophils (red: Ly6g, blue: DAPI). F4/80: Immunofluorescence staining of F4/80 showed macrophages (red: F4/80, blue: DAPI). **B**: ImageJ immunofluorescence profile analysis showed the $CD4^+$, Ly6g, and F4/80 positive scores (n = 6 samples). **C**: Real-time PCR results exhibited chemokine and proinflammatory factors (n = 3 samples). *p<0.05, **p<0.001, two-way analysis of variance (ANOVA). Scale bars: (**A**) 40 μm. *p<0.05, **p<0.01, ***p<0.0001.

antibodies (1:200, Thermo Fisher Scientific, Rockford, IL) and 4'6-diamidino-2-phenylindole (DAPI; 1:500, Beyotime Biotechnology, Shanghai, China). Sections were sliced and immunostained with F4/80 (1:100, Affymetrix, Inc., San Diego, CA), Ly6g (1:100, Biolegend, CA), and $CD4^+$ (1:100, Affymetrix, Inc.). A laser confocal microscope (Olympus) was used to view the images. The immunofluorescence results were analyzed using ImageJ (National Institutes of Health, Bethesda, MA) software.

Oil Red O staining: All 6-mm-thick frozen sections were covered with 4% paraformaldehyde (Solarbio) for 25 min and rinsed twice with PBS for 5 min each time. The sections were stained with filterable Oil Red O (storage liquid:distilled water = 3:2, Cyagen Biosciences Inc.) for 30 min. They were then rinsed three times with PBS for 5 min each time. Following this, the sections were stained with Mayer's hematoxylin (Sigma) for 1 min and washed with water for 3 min. Glycerol (Servicebio, Wuhan, China) was used for the gelatin sealing piece. Six different visual fields were selected from each group, and the positive density of the images was quantitatively analyzed using ImageJ.

Real-time PCR: The GeneJET RNA Purification Kit (Thermo Fisher Scientific, Ottawa, Canada) was used for the isolation of total RNA. The specific primers for detection of *CXCL1*, *CXCL2*, *CCL5*, *CPT1α*, *CPT2*, *PPARα*, *MCP-1*, *IL-1β*, *IL-6*, *TNF-α*, and *GAPDH* were designed and synthesized by Invitrogen (Shanghai, China). The cDNAs of each sample were synthesized using a PrimeScript RT reagent kit (TaKaRa, Tokyo, Japan). Quantitative PCR was conducted using SYBR Green (Vazyme, Nanjing, China) and a Bio-Rad CFX 96

Machine (Bio-Rad, Hercules, CA). The expression levels of each mRNA were normalized to glyceraldehyde-3-phosphate dehydrogenase (GAPDH) expression levels. The relative expression level was calculated using the $2^{-\Delta\Delta CT}$ method. The primers are listed in Table 1.

Western blot analysis: Lacrimal gland tissue was extracted with Radioimmunoprecipitation Assay (RIPA) Lysis Buffer (Beyotime) mixed with phenylmethylsulfonyl fluoride (PMSF; Solarbio). Protein extracts were resolved via 10% sodium dodecyl sulfate–polyacrylamide gel electrophoresis (SDS–PAGE; EPizyme, Shanghai, China) and then electro-transferred to a polyvinylidene difluoride membrane. After blocking, the membranes were probed with primary antibodies to AQP5 (1:2000, Abcam), α-SMA (1:2000, Abcam), GAPDH (1:3000, Kangchen, Shanghai, China), CHOP (1:500, Affinity Biosciences, Wuhan, China), Bax (1:1000, Affinity Biosciences), Bcl-2 (1:2000, Affinity Biosciences), Caspase12 (1:1000, Affinity Biosciences), and GRP78 (1:1000, Affinity Biosciences). Horseradish peroxidase–conjugated secondary antibodies were used, and the bands were developed using a Western Bright Electrochemiluminescence (ECL) substrate (Applygen, Beijing, China). GAPDH was used for normalization of expression [34].

Statistical analysis: All data are presented as the mean ± standard deviation (SD). One-way analysis of variance (ANOVA) was applied to evaluate the significance between different groups, and $p<0.05$ was considered statistically significant. The statistical analysis was performed with Prism software version 8.0 (GraphPad Software, La Jolla, CA).

RESULTS

AQP5 deficiency induced dry eye–like characteristics: Immunofluorescence staining showed that AQP5 was normally expressed in the apical membrane of acinar cells in the lacrimal glands of $AQP5^{+/+}$ mice (Figure 1A). Immunofluorescence staining and western blot demonstrated that no expression of AQP5 was detected in the lacrimal glands of $AQP5^{-/-}$ mice (Figure 1A,B). We found that there was no significant difference in body weight between the two groups (1 month old, $p = 0.5806$; 6 months old, $p = 0.2528$; $n = 10$ per group; Figure 1C). The weight of the lacrimal gland was greater in the 1- and 6-month-old $AQP5^{-/-}$ mice than it was in the age-matched $AQP5^{+/+}$ mice (Figure 1D,E). The tear volume of $AQP5^{-/-}$ mice was significantly lower than that of $AQP5^{+/+}$ mice (Figure 1F). Spontaneous punctate corneal epithelial defects in $AQP5^{-/-}$ mice were observed under a slit lamp (Figure 1G).

AQP5 deficiency induced ultrastructural abnormalities and ER stress in the lacrimal gland: TEM images confirmed that the number and structure of organelles in the lacrimal

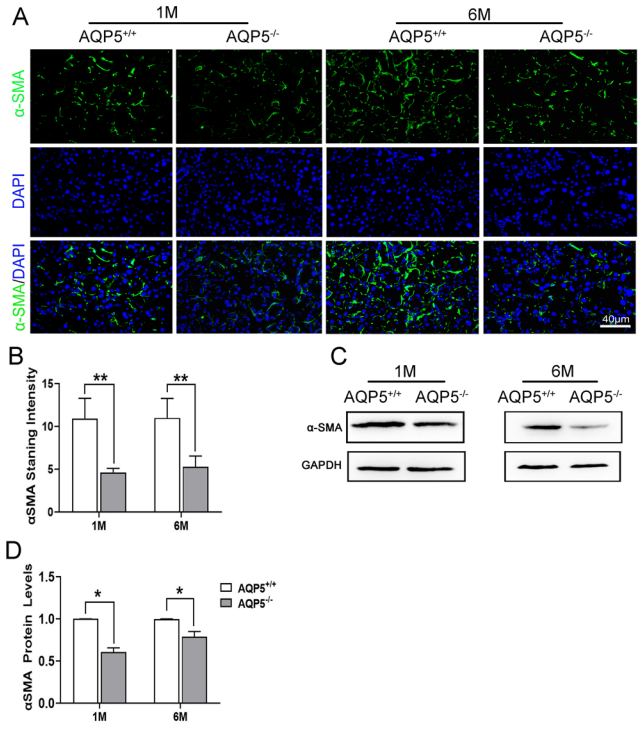

Figure 5. AQP5 deficiency induced structural damage to lacrimal gland myoepithelial cells (MECs) in mice. **A**: Immunofluorescence staining of alpha-smooth muscle actin (α-SMA) showed myoepithelium morphology (green: α-SMA; blue: 4'6-diamidino-2-phenylindole [DAPI]). **B**: ImageJ and GraphPad were used to calculate the result of A (n = 6 samples). **C**: Western blotting showed the expression level of α-SMA and GAPDH in lacrimal glands. **D**: ImageJ and GraphPad were used to compute the result of C (n = 3 samples). Data were expressed as mean ± standard deviation (SD). *p<0.05, **p<0.001 two-way analysis of variance (ANOVA). Scale bars: (**A**) 10 μm, 2 μm. (**D**) 40 μm.

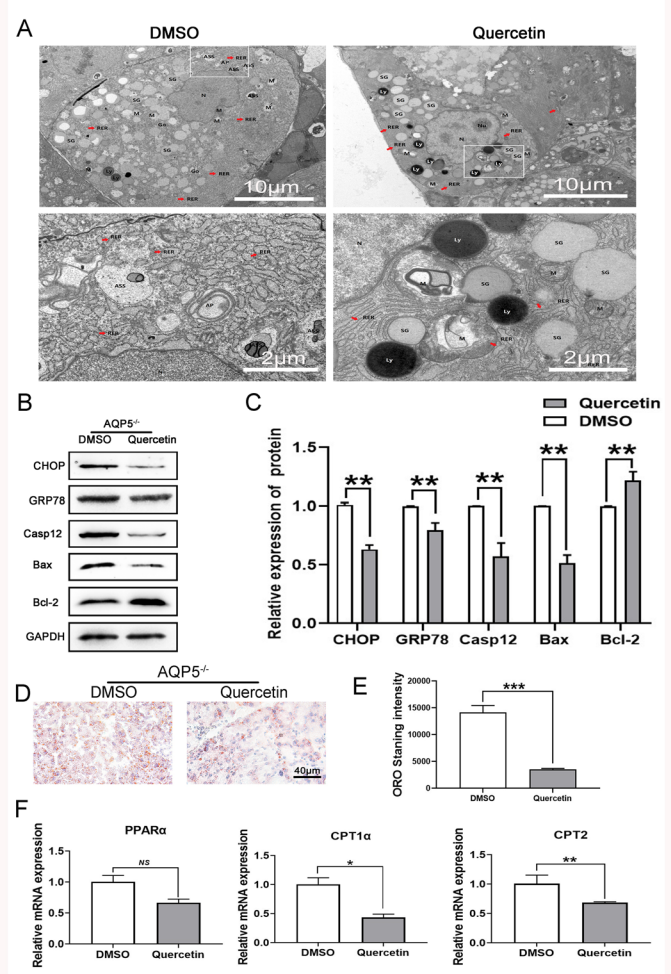

Figure 6. Quercetin relieved endoplasmic reticulum (ER) stress and abnormal lipid metabolism in AQP5$^{-/-}$ mice. **A**: Transmission electron microscopy (TEM) shows the ultrastructure of the acinar cells. **B**: Western blot bands for CHOP, GRP78, Caspase12, Bax, Bcl-2, and GAPDH. **C**: Quantified intensities of western blot bands for CHOP, GRP78, Caspase12, Bax, and Bcl-2 compared with GAPDH (n = 3 samples). **D**: Oil Red O (ORO) staining. **E**: ORO staining intensity was analyzed by ImageJ software (n = 6 samples). **F**: Real-time PCR analysis showed *PPARα*, *CPT1α*, and *CPT2* expression (n = 3 samples). *p<0.05, **p<0.01, **" in line 10 on page 22 to "*p<0.05, **p<0.001, ***p<0.0001.

glands of AQP5$^{+/+}$ mice were normal. Rough ER was dilated and mostly short, and the amount of rough ER was lower in the lacrimal glands of AQP5$^{-/-}$ mice (Figure 2A). To explore the underlying mechanisms of AQP5 deficiency affecting structural ER changes, we investigated whether AQP5 regulated ER stress in the lacrimal gland. The ER stress markers GRP78 and transcription factor CHOP were elevated in the lacrimal glands, suggesting that excessive ER stress was induced by AQP5 deficiency. We also detected ER stress-mediated apoptosis in AQP5$^{-/-}$ mice. The results showed that cleaved Caspase12, a caspase that activates ER stress-mediated apoptosis, was heightened in AQP5$^{-/-}$ mice (Figure 2B,C). We also found that the expression of the apoptosis regulator Bax was increased in AQP5$^{-/-}$ mice (Figure 2B,C). In contrast, the expression of Bcl-2, a cellular protein that inhibits apoptosis, decreased significantly in AQP5$^{-/-}$ mice (Figure 2B,C).

AQP5$^{-/-}$ induced abnormal lipid metabolism in the lacrimal gland: Using Oil Red O staining, an accumulation of neutral triglycerides in the acinar of AQP5$^{-/-}$ mice was observed (Figure 3A). The intensity increased from 1,545.55 ± 523.97 (1 month) and 5,769.42 ± 1,140.71 (6 months) in AQP5$^{+/+}$ mice to 4,365.87 ± 1,383.92 (1 month) and 8,532.98 ± 1,590.97 (6 months) in AQP5$^{-/-}$ mice (n = 6 per group; Figure 3A,B). Real-time PCR was performed with lipid metabolism genes *PPAR*, *CPT1α*, and *CPT2*. It was found that *PPARα* and *CPT1α* were downregulated in the lacrimal glands of 1- and 6-month-old AQP5$^{-/-}$ mice compared with age-matched AQP5$^{+/+}$ mice (n = 3 per group; Figure 3C,D). *CPT2* was downregulated in the lacrimal glands of 1-month-old AQP5$^{-/-}$ old mice (n = 3 per group; Figure 3E).

AQP5 deficiency induced inflammatory cell infiltration in the lacrimal gland: Inflammatory cells infiltrated around the blood vessels in the lacrimal gland of 6-month-old AQP5$^{-/-}$ mice (Figure 4Ai). Immunofluorescence staining identified time-dependent increases in CD4^{+} T lymphocyte density around the acini in lacrimal glands of 1- and 6-month-old AQP5$^{-/-}$ mice compared with the age-matched AQP5$^{+/+}$ mice

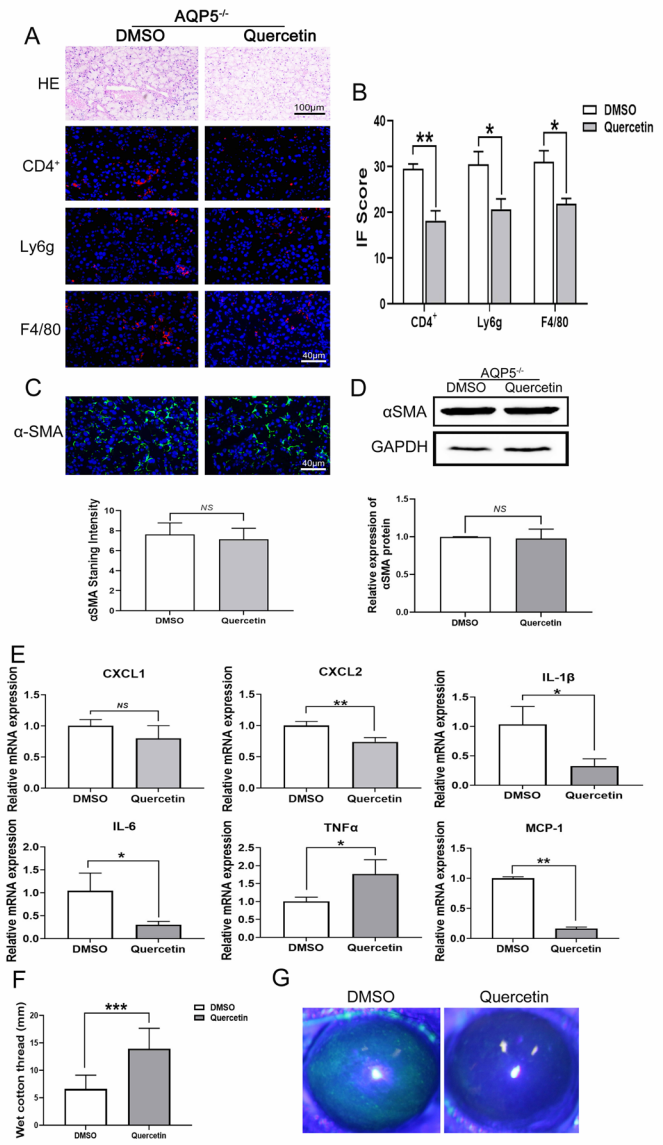

Figure 7. Quercetin alleviated lacrimal gland inflammation caused by AQP5 deficiency. **A**: Hematoxylin and eosin (H&E) staining showed morphological changes. CD4+: Immunofluorescence staining of CD4+ demonstrated CD4+ T cells (red: CD4+, blue: 4'6-diamidino-2-phenylindole [DAPI]). Ly6g: Immunofluorescence staining of Ly6g showed neutrophils (red: Ly6g, blue: DAPI). F4/80: Immunofluorescence staining of F4/80 showed macrophages (red: F4/80, blue: DAPI). **B**: ImageJ immunofluorescence profile analysis showed the CD4+ positive score, Ly6g positive score, and mean fluorescence intensity of F4/80 (n = 6 samples). **C**: Immunofluorescence staining of alpha-smooth muscle actin (α-SMA) showed myoepithelium morphology (green: α-SMA, blue: DAPI), and ImageJ and GraPade were used to compute the result (n = 6 samples). **D**: Western blotting showed the expression level of α-SMA and GAPDH (n = 3 samples). **E**: Real-time PCR exhibits expression of chemokine and proinflammatory factors (n = 3 samples). **F**: The lacrimal secretion of AQP5$^{-/-}$ mice was measured using the phenol red cotton thread method. **G**: Sodium fluorescein staining in the cornea. *p<0.05, **p<0.001. Independent sample t test. Scale bars: (**A**): 100 μm, 40 μm. *p<0.05, **p<0.01, ***p<0.0001.

(Figure 4Aii,Bi). Neutrophil infiltration identified by Ly6g staining increased in the lacrimal gland of 6-month-old AQP5$^{-/-}$ mice (Figure 4Aiii,Bii). F4/80 staining increased the mononuclear macrophage density in the lacrimal gland in 1- and 6-month-old AQP5$^{-/-}$ mice (Figure 4Aiv,Biii). Expression of proinflammatory factors, such as *IL-6*, *IL-1β*, *MCP-1*, and *TNF-α*, significantly increased in the lacrimal glands of 1- and 6-month-old AQP5$^{-/-}$ mice compared with the age-matched AQP5$^{+/+}$ mice (Figure 4C). In parallel, chemokine *CXCL1*, *CXCL2*, and *CCL5* expression levels significantly increased in 1- and 6-month-old AQP5$^{-/-}$ mice (Figure 4C).

AQP5 deficiency induced structural MEC damage in the lacrimal gland: α-SMA is a MEC marker [35]. In this study, α-SMA expression showed an obvious decline in the lacrimal glands of AQP5$^{-/-}$ mice (Figure 5A). According to the analysis of α-SMA staining, the intensity decreased from 10.93 ± 0.76 (1 month) and 10.99 ± 2.52 (6 months) of AQP5$^{+/+}$ mice to 4.63 ± 0.46 (1 month) and 5.29 ± 1.25 (6 months) of AQP5$^{-/-}$ mice (n = 6 per group; Figure 5B). Downregulation of α-SMA was further confirmed by western blot in AQP5$^{-/-}$ mice (p<0.05; n = 3 per group; Figure 5C,D).

Quercetin alleviated ER stress and abnormal lipid metabolism: TEM images confirmed that the rough ER was abundant

and orderly, with many ribosomes attached to its surface in the lacrimal glands of the quercetin group. There was a lot of ER retained, and more floccules were found in the reticulum pool in the lacrimal gland of the DMSO group (Figure 6A). More importantly, the intraperitoneal injection of quercetin significantly attenuated the expression of GRP78, CHOP, Caspase12, and Bax ($p<0.005$, n = 3 per group; Figure 6B,C). In contrast, the expression of Bcl-2 increased significantly, reaching 1 ± 0.001 for the DMSO group and 1.21 ± 0.076 for the quercetin group (Figure 6B,C). Lipid accumulation slightly decreased, with Oil Red O staining density observed at 14,118.8 ± 1,307.11 for the DMSO group and 3,484.38 ± 198.71 for the quercetin group (Figure 6D,E). Real-time PCR confirmed that the mRNA levels of *PPARα*, *CPT1α* ($p<0.05$, n = 3 per group), and *CPT2* ($p<0.005$, n = 3 per group) were downregulated in the lacrimal glands of the quercetin group compared with the DMSO group (Figure 6F).

Quercetin reduced the inflammation caused by AQP5 deficiency: Compared with the DMSO group, the quercetin group showed less inflammatory infiltration in the lacrimal epithelial cells (Figure 7Ai,B). Instead, numbers of inflammatory cells, such as neutrophils, macrophages, and $CD4^+$ T cells, fell significantly with quercetin treatment (Figure 7Aii-iv,B). Immunofluorescence staining and western blot analysis showed that quercetin had no significant effect on the expression levels of α-SMA (Figure 7C,D). Proinflammatory factors *IL-6*, *IL-1β*, *MCP-1*, and *TNF-α* were downregulated; *CXCL2*, a chemokine, was also significantly downregulated in the lacrimal glands of the quercetin group (n = 3 per group; Figure 7E). The tear volume increased from 6.625 ± 2.501 in the DMSO group to 13.938 ± 3.746 in the quercetin group ($p<0.05$, n = 6 per group; Figure 7F). Under a slit lamp, it was found that quercetin partially alleviated punctate epithelial defects in the corneas of $AQP5^{-/-}$ mice (Figure 7G).

Table 2. The gene information.

Gene	Gene ID	OMIM
CPT1α	12894	138420
CPT2	12896	600650
PPARα	19015	170998
MCP-1	20296	601159
CXCL1	14825	155730
CXCL2	20310	139110
CCL5	20311	187011
IL-1β	16176	147720
IL-6	16193	147620
TNF-α	21926	191160
GAPDH	14433	138400

DISCUSSION

The tear film's aqueous layer is mainly secreted by the lacrimal gland. Many factors related to tears and the ocular surface can cause dry eye, usually accompanied by increased osmolarity of the tear film and ocular surface inflammation. Dry eyes can cause eye discomfort, visual impairment, tear film instability, and potential damage to the ocular surface [36]. It is known that the popularization of air conditioning, frequent usage of visual display terminals, and increase in wearers of soft contact lenses may all be associated with a rise in the incidence of dry eye [37].

Abnormal AQP5 trafficking in SS may contribute to decreased lacrimation and dry eye in patients [38]. A missense mutation in AQP5 (p.G308A) probably resulted in abnormal membrane insertion or ineffective trafficking. Rats with this mutation show extremely low water secretion from their salivary glands [39]. In our previous study, we found that $AQP5^{-/-}$ mice naturally develop dry eye symptoms. However, the mechanism by which the loss of AQP5 protein induces dry eye in mice remains unclear. To explore the exact mechanism of the decrease in tear secretion caused by AQP5 deficiency, we analyzed its ultrastructure. Rough ER in the lacrimal gland cells of $AQP5^{-/-}$ mice was slightly dilated and mostly short, and ribosomes were attached to it without shedding.

Prolonged or severe ER stress affects the function and structure of proteins and lipids [40,41]. ER stress–induced inflammation in the lacrimal glands plays an important role in the pathogenesis of dry eye syndrome or SS [42]. Thus, ER stress can potentially serve as a target for treating dry eye. Our results indicated that the lacrimal glands of $AQP5^{-/-}$ mice undergo more severe ER stresses than normal lacrimal glands do. AQP5 deficiency increased the levels of CHOP, GRP78, and Bax while decreasing Bcl-2 expression. CHOP is an ER stress–specific nuclear transcription factor. GRP78, a calcium ion binding molecule located in the ER, shows marker upregulation in ER chaperones in response to ER stress [43]. In contrast, Bcl-2 is a cellular protein that inhibits apoptosis. ER stress induces Caspase12-mediated apoptotic cell death [44]. Our western blot results showed a high expression of cleaved Caspase12 in $AQP5^{-/-}$ mice. However, low expression of the cleaved Caspase12 protein was observed in the normal lacrimal glands.

In dry eye, ER stress induces abnormal lipid metabolism and various inflammatory and apoptotic pathways, leading to lacrimal gland cell death [45]. We found that lipid droplets accumulated along with changes of *PPARα, CPT1α*, and *CPT2* in $AQP5^{-/-}$ mice. We also found that ER stress activated inflammatory signaling pathways based on increases in inflammatory cell infiltration. Expression levels

of proinflammatory factors, such as *IL-6*, *IL-1β*, *MCP-1*, and *TNF-α* significantly increased in the lacrimal glands of 1- and 6-month-old AQP5$^{-/-}$ mice compared with the age-matched AQP5$^{+/+}$ mice. It is presumed that ER stress induces lipid deposition in acinar cells and the surrounding microenvironment. ER stress also activated inflammation, which induced acinar cell apoptosis, as reported previously [45].

Decreased aqueous tear secretion could develop as a consequence of several pathological changes in AQP5$^{-/-}$ mice. First, lipid deposition induced by ER stress compromises cell function [46,47]. Second, infiltration of inflammatory cells disrupts acinar cells [48,49]. Third, the inflammatory cytokines secreted by infiltrated inflammatory cells directly reduce aqueous secretion of acinar cells [50]. Finally, MECs exert pressure on the acinus and promote tear secretion [51,52]. Our results indicate that the MEC structure became disordered and disrupted in AQP5$^{-/-}$ mice. These pathological changes are likely to account for how AQP5 deficiency reduces aqueous tear secretion.

Quercetin is a natural product with antioxidative properties [53,54]. It has been shown to inhibit mitochondrial dysfunction and inflammation in osteoarthritis animal models [55,56]. Moreover, it has been found that 0.5% quercetin eye drops aid in increasing tear volumes. Quercetin treatment can also increase the density of goblet cells [28]. Our results indicated that quercetin alleviated ER stress by attenuating the expression of GRP78, CHOP, Caspase12, and Bax. Our findings revealed that quercetin alleviated lipid accumulation in AQP5$^{-/-}$ mice via downregulated expression of *CPT1α* and *CPT2*. We also found that quercetin reduced inflammatory cell infiltration and proinflammatory factor expression.

In summary, AQP5 deficiency induced severe ER stress and inhibited fatty acid clearance in the lacrimal gland. Losses in structural integrity and declines in fluid secretion are consistent with proinflammatory cytokine upregulation and inflammatory cell infiltration. Quercetin indeed reduced inflammation and lipid deposition, while it partially ameliorated declines in lacrimal gland tear secretion. These results suggest that quercetin may provide therapeutic benefits in dry eye induced by AQP5 deficiency.

ACKNOWLEDGMENTS

This work was supported by the National Natural Science Foundation of China (No. 81970782, No. 81600721), Shandong Provincial Natural Science Foundation (No. ZR2018MH016), Qingdao Postdoctoral Application Research Project (No. 40518060071), China Postdoctoral Science Foundation (No. 2017M612211).

REFERENCES

1. Bannier-Hélaouët M, Post Y, Korving J, Trani Bustos M, Gehart H, Begthel H, Bar-Ephraim YE, van der Vaart J, Kalmann R, Imhoff SM, Clevers H. Exploring the human lacrimal gland using organoids and single-cell sequencing. Cell Stem Cell 2021; 28:1221-32.e7. [PMID: 33730555].

2. Klećkowska-Nawrot J, Goździewska-Harłajczuk K, Kowalczyk A, Łukaszewicz E, Nowaczyk R. Histological, histochemical and ultrastructural studies on Harderian and lacrimal glands of the Capercaillie (Tetrao urogallus major L.). Acta Biol Hung 2016; 67:27-41. [PMID: 26960354].

3. Hodges RR, Dartt DA. Regulatory pathways in lacrimal gland epithelium. Int Rev Cytol 2003; 231:129-96. [PMID: 14713005].

4. Botelho SY. TEARS AND THE LACRIMAL GLAND. Sci Am 1964; 211:78-86. [PMID: 14216948].

5. Sullivan DA, Wickham LA, Rocha EM, Krenzer KL, Sullivan BD, Steagall R, Cermak JM, Dana MR, Ullman MD, Sato EH, Gao J, Rocha FJ, Ono M, Silveira LA, Lambert RW, Kelleher RS, Tolls DB, Toda I. Androgens and dry eye in Sjögren's syndrome. Ann N Y Acad Sci 1999; 876:312-24. [PMID: 10415627].

6. Brito-Zerón P, Retamozo S, Kostov B, Baldini C, Bootsma H, De Vita S, Dörner T, Gottenberg JE, Kruize AA, Mandl T, Ng WF, Seror R, Tzioufas AG, Vitali C, Bowman S, Mariette X, Ramos-Casals M. Efficacy and safety of topical and systemic medications: a systematic literature review informing the EULAR recommendations for the management of Sjögren's syndrome. RMD Open. 2019; 5:e001064-[PMID: 31749986].

7. Yaguchi S, Ogawa Y, Kawakita T, Shimmura S, Tsubota K. Tissue Renin-Angiotensin System in Lacrimal Gland Fibrosis in a Murine Model of Chronic Graft-Versus-Host Disease. Cornea 2015; 34:Suppl 11S142-52. [PMID: 26448172].

8. Liu Y, Hirayama M, Kawakita T, Tsubota K. A Ligation of the Lacrimal Excretory Duct in Mouse Induces Lacrimal Gland Inflammation with Proliferative Cells. Stem Cells Int 2017; 2017:4923426-[PMID: 28874911].

9. Rocha EM, Alves M, Rios JD, Dartt DA. The aging lacrimal gland: changes in structure and function. Ocul Surf 2008; 6:162-74. [PMID: 18827949].

10. Bravo R, Parra V, Gatica D, Rodriguez AE, Torrealba N, Paredes F, Wang ZV, Zorzano A, Hill JA, Jaimovich E, Quest AF, Lavandero S. Endoplasmic reticulum and the unfolded protein response: dynamics and metabolic integration. Int Rev Cell Mol Biol 2013; 301:215-90. [PMID: 23317820].

11. Hotamisligil GS. Endoplasmic reticulum stress and the inflammatory basis of metabolic disease. Cell 2010; 140:900-17. [PMID: 20303879].

12. Minamino T, Komuro I, Kitakaze M. Endoplasmic reticulum stress as a therapeutic target in cardiovascular disease. Circ Res 2010; 107:1071-82. [PMID: 21030724].

13. Coursey TG, Tukler Henriksson J, Barbosa FL, de Paiva CS, Pflugfelder SC. Interferon-γ-Induced Unfolded Protein Response in Conjunctival Goblet Cells as a Cause of Mucin Deficiency in Sjögren Syndrome. Am J Pathol 2016; 186:1547-58. [PMID: 27085137].

14. Roen JL, Stasior OG, Jakobiec FA. Aging changes in the human lacrimal gland: role of the ducts. The CLAO journal: official publication of the Contact Lens Association of Ophthalmologists Inc 1985; 11:237-42. .

15. Liu HH, Li JJ. Aging and dyslipidemia: a review of potential mechanisms. Ageing Res Rev 2015; 19:43-52. [PMID: 25500366].

16. Das N, Mandala A, Naaz S, Giri S, Jain M, Bandyopadhyay D, Reiter RJ, Roy SS. Melatonin protects against lipid-induced mitochondrial dysfunction in hepatocytes and inhibits stellate cell activation during hepatic fibrosis in mice. J Pineal Res 2017; 62:e12404-[PMID: 28247434].

17. Erbay E, Babaev VR, Mayers JR, Makowski L, Charles KN, Snitow ME, Fazio S, Wiest MM, Watkins SM, Linton MF, Hotamisligil GS. Reducing endoplasmic reticulum stress through a macrophage lipid chaperone alleviates atherosclerosis. Nat Med 2009; 15:1383-91. [PMID: 19966778].

18. Katsiougiannis S, Tenta R, Skopouli FN. Endoplasmic reticulum stress causes autophagy and apoptosis leading to cellular redistribution of the autoantigens Ro/Sjögren's syndrome-related antigen A (SSA) and La/SSB in salivary gland epithelial cells. Clin Exp Immunol 2015; 181:244-52. [PMID: 25845745].

19. He X, Zhao Z, Wang S, Kang J, Zhang M, Bu J, Cai X, Jia C, Li Y, Li K, Reinach PS, Quantock AJ, Liu Z, Li W. High-Fat Diet-Induced Functional and Pathologic Changes in Lacrimal Gland. Am J Pathol 2020; 190:2387-402. [PMID: 32919976].

20. Takata K, Matsuzaki T, Tajika Y. Aquaporins: water channel proteins of the cell membrane. Prog Histochem Cytochem 2004; 39:1-83. [PMID: 15242101].

21. Hasegawa T, Azlina A, Javkhlan P, Yao C, Akamatsu T, Hosoi K. Novel phosphorylation of aquaporin-5 at its threonine 259 through cAMP signaling in salivary gland cells. Am J Physiol Cell Physiol 2011; 301:C667-78. [PMID: 21633078].

22. Ma T, Song Y, Gillespie A, Carlson EJ, Epstein CJ, Verkman AS. Defective secretion of saliva in transgenic mice lacking aquaporin-5 water channels. J Biol Chem 1999; 274:20071-4. [PMID: 10400615].

23. Krane CM, Melvin JE, Nguyen HV, Richardson L, Towne JE, Doetschman T, Menon AG. Salivary acinar cells from aquaporin 5-deficient mice have decreased membrane water permeability and altered cell volume regulation. J Biol Chem 2001; 276:23413-20. [PMID: 11290736].

24. Sánchez de Medina F, Gálvez J, Romero JA, Zarzuelo A. Effect of quercitrin on acute and chronic experimental colitis in the rat. J Pharmacol Exp Ther 1996; 278:771-9. [PMID: 8768730].

25. Basarkar PW, Nath N. Hypocholesterolemic and hypolipidemic activity of quercetin–a vitamin P-like compound in rats. Indian J Med Res 1983; 77:122-6. [PMID: 6862537].

26. Sen CK, Packer L. Antioxidant and redox regulation of gene transcription. FASEB J 1996; 10:709-20. [PMID: 8635688].

27. Gloire G, Legrand-Poels S, Piette J. NF-kappaB activation by reactive oxygen species: fifteen years later. Biochem Pharmacol 2006; 72:1493-505. [PMID: 16723122].

28. Oh HN, Kim CE, Lee JH, Yang JW. Effects of Quercetin in a Mouse Model of Experimental Dry Eye. Cornea 2015; 34:1130-6. [PMID: 26203745].

29. McKay TB, Karamichos D. Quercetin and the ocular surface: What we know and where we are going. Exp Biol Med (Maywood) 2017; 242:565-72. [PMID: 28056553].

30. Miles SL, McFarland M, Niles RM. Molecular and physiological actions of quercetin: need for clinical trials to assess its benefits in human disease. Nutr Rev 2014; 72:720-34. [PMID: 25323953].

31. Cai X, Bao L, Dai X, Ding Y, Zhang Z, Li Y. Quercetin protects RAW264.7 macrophages from glucosamine-induced apoptosis and lipid accumulation via the endoplasmic reticulum stress pathway. Mol Med Rep 2015; 12:7545-53. [PMID: 26398703].

32. Tang S, Di G, Hu S, Liu Y, Dai Y, Chen P. AQP5 regulates vimentin expression via miR-124–3p.1 to protect lens transparency. Exp Eye Res 2021; 205:108485-[PMID: 33582182].

33. Liu Y, Di G, Hu S, Zhao T, Xu X, Wang X, Chen P. Expression Profiles of CircRNA and mRNA in Lacrimal Glands of AQP5($^{-/-}$) Mice With Primary Dry Eye. Front Physiol 2020; 11:1010-[PMID: 33013441].

34. Yu C, Chen P, Xu J, Liu Y, Li H, Wang L, Di G. hADSCs derived extracellular vesicles inhibit NLRP3inflammasome activation and dry eye. Sci Rep 2020; 10:14521-[PMID: 32884023].

35. Wang YL, Tan Y, Satoh Y, Ono K. Morphological changes of myoepithelial cells of mouse lacrimal glands during postnatal development. Histol Histopathol 1995; 10:821-7. [PMID: 8574002].

36. Lemp MA, Baudouin C, Baum J, Dogru M, Foulks GN, Kinoshita SP, Laibson P, Mcculley J, Murube J, Pflugfelder SC. The definition and classification of dry eye disease: report of the Definition and Classification Subcommittee of the International Dry Eye WorkShop (2007). Ocul Surf 2007; 5:75-92. [PMID: 17508116].

37. Shinomiya K, Ueta M, Kinoshita S. A new dry eye mouse model produced by exorbital and intraorbital lacrimal gland excision. Sci Rep 2018; 8:1483-[PMID: 29367638].

38. Tsubota K, Hirai S, King LS, Agre P, Ishida N. Defective cellular trafficking of lacrimal gland aquaporin-5 in Sjögren's syndrome. Lancet (London, England) 2001; 357:688-9. [PMID: 11247557].

39. Murdiastuti K, Purwanti N, Karabasil MR, Li X, Yao C, Akamatsu T, Kanamori N, Hosoi K. A naturally occurring point mutation in the rat aquaporin 5 gene, influencing its protein production by and secretion of water from salivary glands. Am J Physiol Gastrointest Liver Physiol 2006; 291:G1081-8. [PMID: 16901987].

40. Luoma PV. Elimination of endoplasmic reticulum stress and cardiovascular, type 2 diabetic, and other metabolic diseases. Ann Med 2013; 45:194-202. [PMID: 22928964].

41. Ron D, Walter P. Signal integration in the endoplasmic reticulum unfolded protein response. Nat Rev Mol Cell Biol 2007; 8:519-29. [PMID: 17565364].

42. Baban B, Liu JY, Abdelsayed R, Mozaffari MS. Reciprocal relation between GADD153 and Del-1 in regulation of salivary gland inflammation in Sjögren syndrome. Exp Mol Pathol 2013; 95:288-97. [PMID: 24060278].

43. Rao RV, Peel A, Logvinova A, del Rio G, Hermel E, Yokota T, Goldsmith PC, Ellerby LM, Ellerby HM, Bredesen DE. Coupling endoplasmic reticulum stress to the cell death program: role of the ER chaperone GRP78. FEBS Lett 2002; 514:122-8. [PMID: 11943137].

44. Shiraishi H, Okamoto H, Yoshimura A, Yoshida H. ER stress-induced apoptosis and caspase-12 activation occurs downstream of mitochondrial apoptosis involving Apaf-1. J Cell Sci 2006; 119:3958-66. [PMID: 16954146].

45. Wang X, Li W, Zhou Q, Li J, Wang X, Zhang J, Li D, Qi X, Liu T, Zhao X, Li S, Yang L, Xie L. MANF Promotes Diabetic Corneal Epithelial Wound Healing and Nerve Regeneration by Attenuating Hyperglycemia-Induced Endoplasmic Reticulum Stress. Diabetes 2020; 69:1264-78. [PMID: 32312869].

46. Feng X, Yu W, Li X, Zhou F, Zhang W, Shen Q, Li J, Zhang C, Shen P. Apigenin, a modulator of PPARγ, attenuates HFD-induced NAFLD by regulating hepatocyte lipid metabolism and oxidative stress via Nrf2 activation. Biochem Pharmacol 2017; 136:136-49. [PMID: 28414138].

47. Spahis S, Delvin E, Borys JM, Levy E. Oxidative Stress as a Critical Factor in Nonalcoholic Fatty Liver Disease Pathogenesis. Antioxid Redox Signal 2017; 26:519-41. [PMID: 27452109].

48. Bron AJ, de Paiva CS, Chauhan SK, Bonini S, Gabison EE, Jain S, Knop E, Markoulli M, Ogawa Y, Perez V, Uchino Y, Yokoi N, Zoukhri D, Sullivan DA. TFOS DEWS II pathophysiology report. Ocul Surf 2017; 15:438-510. [PMID: 28736340].

49. Damato BE, Allan D, Murray SB, Lee WR. Senile atrophy of the human lacrimal gland: the contribution of chronic inflammatory disease. Br J Ophthalmol 1984; 68:674-80. [PMID: 6331845].

50. Aluri HS, Kublin CL, Thotakura S, Armaos H, Samizadeh M, Hawley D, Thomas WM, Leavis P, Makarenkova HP, Zoukhri D. Role of Matrix Metalloproteinases 2 and 9 in Lacrimal Gland Disease in Animal Models of Sjögren's Syndrome. Invest Ophthalmol Vis Sci 2015; 56:5218-28. [PMID: 26244298].

51. Lemullois M, Rossignol B, Mauduit P. Immunolocalization of myoepithelial cells in isolated acini of rat exorbital lacrimal gland: cellular distribution of muscarinic receptors. Biol Cell 1996; 86:175-81. [PMID: 8893507].

52. Makarenkova HP, Dartt DA. Myoepithelial Cells: Their Origin and Function in Lacrimal Gland Morphogenesis, Homeostasis, and Repair. Curr Mol Biol Rep. 2015; 1:115-23. [PMID: 26688786].

53. de Oliveira MR, Nabavi SM, Braidy N, Setzer WN, Ahmed T, Nabavi SF. Quercetin and the mitochondria: A mechanistic view. Biotechnol Adv 2016; 34:532-49. [PMID: 26740171].

54. Roslan J, Giribabu N, Karim K, Salleh N. Quercetin ameliorates oxidative stress, inflammation and apoptosis in the heart of streptozotocin-nicotinamide-induced adult male diabetic rats. Biomed Pharmacother 2017; 86:570-82. [PMID: 28027533].

55. Qiu L, Luo Y, Chen X. Quercetin attenuates mitochondrial dysfunction and biogenesis via upregulated AMPK/SIRT1 signaling pathway in OA rats. Biomed Pharmacother 2018; 103:1585-91. [PMID: 29864946].

56. Wei B, Zhang Y, Tang L, Ji Y, Yan C, Zhang X. Protective effects of quercetin against inflammation and oxidative stress in a rabbit model of knee osteoarthritis. Drug Dev Res 2019; 80:360-7. [PMID: 30609097].

Articles are provided courtesy of Emory University and the Zhongshan Ophthalmic Center, Sun Yat-sen University, P.R. China. The print version of this article was created on 7 December 2021. This reflects all typographical corrections and errata to the article through that date. Details of any changes may be found in the online version of the article.